HOW GOOD IS THE COLLECTIVE MODEL?

G. BERTSCH and S.F. TSAI*
Department of Physics and Cyclotron Laboratory, Michigan State University, East Lansing, Michigan 48824, USA

Received 18 April 1974

We use Hartree–Fock RPA theories of ^{208}Pb as a testing ground for collective models of the inelastic scattering transition densities. For isoscalar transitions, the standard collective model and the Tassie model both provide excellent descriptions of the transition density to the strongest states. For the isovector dipole mode, we find two states. The lower state has a transition density resembling the Steinwedel–Jensen model, while the upper state has a transition density resembling the Goldhaber–Teller model. The energetics of the collective states, as summarized in heuristicly derived sum rules, are quite close to the results of the RPA calculations.

We have developed a calculational technique for studying inelastic scattering properties of spherical nuclei, using the RPA response in large particle-hole spaces [1,2] with a Hartree–Fock model of the Skyrme type [3]. Much analysis of data has been done using simple collective models for the response, so it is of interest to compare these models with the more detailed Hartree–Fock RPA theories. The most valuable thing provided by a collective model is the shape of the transition densities between ground and excited states. This transition density is the function $\rho_{no}(r)$ defined by

$$Y^L_M(\hat{r})\,\rho_{no}(r) = \langle\psi_o|a^+(r)a(r)|\psi^L_n\rangle$$

where $a^+(r)a(r)$ is the nucleon density operator at point r, and ψ_o and ψ^L_n are ground and excited states of the nucleus.

The simplest collective model for isoscalar excitations, the well-known model of Bohr [4] is based on a classical oscillation of surface position

$$R = R_o(1 + \sum_M^L \beta_L/\sqrt{2L+1}\,Y^L_M(\hat{r})). \tag{1}$$

In this model

$$\rho_{no}(r) = \frac{\beta_L R_o}{\sqrt{2L+1}}\frac{d\rho_o}{dr}, \tag{2}$$

where ρ_o is the density of the ground state.

A second model was derived by Tassie [5] under the assumption that the velocity field in the nuclear vibration is irrotational and incompressible (except for $L = 0$).[‡] The transition density in the Tassie model is given by

$$\begin{aligned}\rho_{no}(r) &= r^{L-1}\,d\rho_o/dr, \qquad L \neq 0\\ &= 3\rho_o + r\,d\rho_o/dr, \qquad L = 0\end{aligned} \tag{3}$$

This model works very well in fitting shapes of inelastic electron scattering [6], and can also be derived from an energy-weighted sum rule and the assumption that a single state exhausts the sum [7,8].

We calculate particle-hole Green's functions in coordinate space. These are related to transition densities by

$$G(r,r',E) = \sum_n \rho_{no}(r)\rho_{no}(r')\left(\frac{1}{E_n-E-i\epsilon} + \frac{1}{E_n+E-i\epsilon}\right) \tag{4}$$

where the sum is over all excited states of the nucleus. Thus a transition density can be extracted from G by

$$\rho_{no}(r) = \sqrt{\epsilon\,\mathrm{Im}\,G(r,r,E_n)} \tag{5}$$

or more practically

* Supported by the National Science Foundation.

‡ These are familiar assumptions in hydrodynamics, so the model is often called the hydrodynamic model. This is a misnomer which becomes evident when the energetics of the vibrations are studied macroscopically [9].

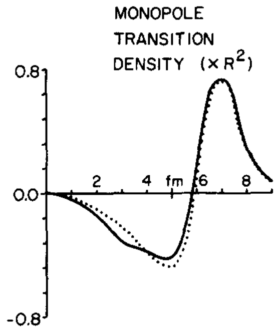

Fig. 1. $T = 0$ monopole transition density ($\times r^2$) in ^{208}Pb, between ground and the 20 MeV giant monopole state. The solid curve is the calculation of eq. (6) with the SkI interaction; the dotted curve is the prediction of the Tassie model, eq. (3), normalized for a visual fit.

$$\rho_{no}(r) = \left[\frac{1}{\pi}\,\mathrm{Im}\int_{E_n-\Delta}^{E_n+\Delta} G(r,r,E)\,\mathrm{d}E\right]^{1/2}. \qquad (6)$$

We use the interactions SkI and SkII defined by Vautherin and Brink [3], generate Hartree–Fock basis, and take the particle-hole configurations going up to 40 MeV excitation. We then calculate the RPA Green's function at the strongest poles, and use eq. (6) to extract the transition densities. Some results for ^{208}Pb using the SkI interaction are shown in figs. 1, 2, and 3, for states of $L = 0, 2$, and 3, respectively. The fits to the collective model are very good. For $L \neq 0$, the Tassie model is somewhat poorer than the standard model. This indicates that the finite compressibility is significant in the nuclear interior. The transition densities for the SkII interaction have virtually identical shapes. We also list in the figure captions the fraction of the energy-weighted sum rule exhausted by the state. The fraction is large for $L = 2$, so we should not be surprised that the Tassie model works here.

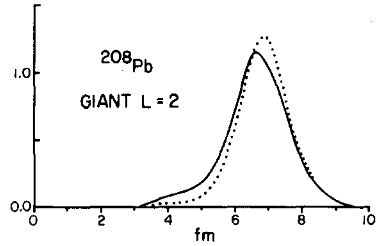

Fig. 2. $T = 0$ quadrupole transition density ($\times r^2$) in ^{208}Pb with the SkI interaction to the giant quadrupole state predicted at 11.0 MeV. This state as given by the RPA calculation exhausts 70% of the energy-weighted isoscalar sum rule. The solid curve is the calculation of eq. (6); the dashed curve is the collective model, eq. (7).

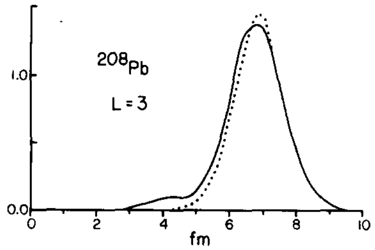

Fig. 3. $T = 0$ octupole transition density ($\times r^2$) in ^{208}Pb from ground to the collective state predicted at 2.7 MeV with the SkI interaction. The RPA calculation gives this state 17% of the energy-weighted isoscalar sum rule. The curves have the same meaning as in fig. 2.

The situation with the isovector dipole mode is entirely different. The picture of incompressible, irrotational flow yields the Goldhaber–Teller model [10], in which

$$\rho_{no}^{\mathrm{GT}}(r) = c\,\mathrm{d}\rho_0/\mathrm{d}r. \qquad (7)$$

This also follows from the sum rule ansatz [7], if the exchange potential in the Hamiltonian is neglected. A competing model for the dipole state was worked out by Steinwedel, Jensen, and Jensen [11], who allow compression of the neutrons and protons separately. The transition density is found to be

$$\rho_{no}^{\mathrm{SJ}}(r) = c' j_1(qr), \qquad r < R$$

with q determined from

$$\frac{\mathrm{d}}{\mathrm{d}r} j_1(qR) = 0, \qquad (8)$$

where R is the nuclear surface radius.

Now let us see which one is more accurate. We find that RPA is very amenable; there are two dipole modes, the lower resembling ρ^{SJ} and the upper resembling ρ^{GT}! This is shown in fig. 4. In fact we find two states in all the nuclei we have examined; in ^{16}O the splitting is due to the spin-orbit potential but in heavier nuclei it is independent of the spin-orbit potential.

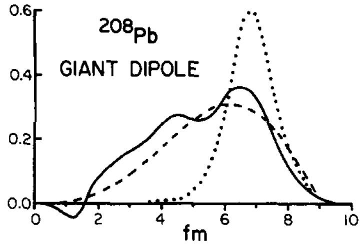

Fig. 4a.

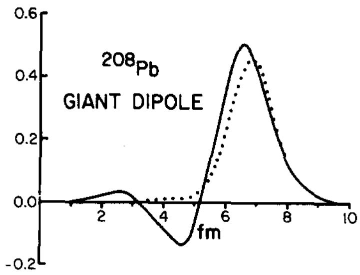

Fig. 4b.

Fig. 4. $T = 1$ dipole transition densities ($\times\, r^2$) to the lower state at 12.2 MeV (fig. 4a) and the upper state at 16.1 MeV (fig. 4b), with SkI interaction. Velocity-dependent terms in the particle-hole interaction are neglected. The dashed curve corresponds to the SJ model, eq. (8), with $q = 0.5\ \mathrm{fm}^{-1}$. The dotted curves are obtained from the GT model, eq. (7). Solid curves represent the RPA result, eq. (6).

Our original calculations with Woods–Saxon wavefunctions and no explicit velocity dependence give the lower peak the preponderance of strength with the upper peak rather small. When the full velocity-dependence of the residual interaction is turned on, the upper peak grows and dominates the strength function. Fig. 4 shows an intermediate situation where two peaks exist, but the GT state does not yet carry the greatest strength. Similar shapes are obtained with the full velocity dependence in the interaction.

Empirically only one state is seen in spherical nuclei heavier than ^{16}O. Thus our results show that the physics of the isovector mode is incorrectly modeled by RPA with strongly velocity-dependent interactions. Perhaps this is not surprising; in these models we attempt to get the full isovector sum rule in a representation containing only simple configurations; it seems likely that a significant part of the sum rule is contained in short-range correlations [12] which could not be represented by 1p–1h states. It is also not surprising that the GT state is the higher one; this is well-known from the predicted A-dependence of the two states.

We now turn to some consideration of the energetics of the isoscalar modes. An approximate sum rule can be derived from the standard energy-weighted sum rule and the collective model. The result is [13]

$$\sum_\alpha E_\alpha^L \frac{(\beta_\alpha^L)^2}{(2L+1)} = L\left(\frac{\hbar^2}{2mR^2}\right)\frac{4\pi}{3A} \tag{9}$$

with the radius of the nucleus R given by

$$R = 1.2\,A^{(1/3)}. \tag{10}$$

To compare with the RPA theory, we define $\beta_\alpha^L(\mathrm{RPA})$ by

$$\frac{(\beta_\alpha^L(\mathrm{RPA}))^2}{(2L+1)} = \frac{\frac{1}{\pi}\int_{E_\alpha-\Delta}^{E_\alpha+\Delta} \mathrm{d}E\ \mathrm{Im}\langle(\mathrm{d}\rho_0/\mathrm{d}r)G(\mathrm{d}\rho_0/\mathrm{d}r)\rangle}{\left[R\int(\mathrm{d}\rho_0/\mathrm{d}r)^2 r^2\mathrm{d}r\right]^2}. \tag{11}$$

We determine the right hand side of eq. (11) numerically, integrating the energy-weighted sum to 40 MeV excitation. This is compared with the sum rule, eq. (9), in fig. 5. We see that the agreement is very good.

Another quantity of importance is the $1/E$-weighted

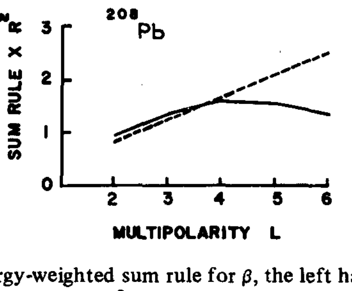

Fig. 5. Energy-weighted sum rule for β, the left hand side of eq. (9), multiplied by R^2, as a function of multipolarity L. The solid curve is calculated from eq. (11), the dashed from eq. (9).

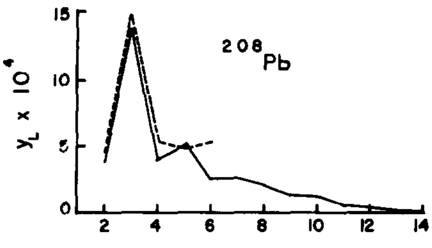

Fig. 6. Core coupling strength Y_L as given by eq. (13) is shown as the solid curve. The dashed curve is taken from table 5 of ref. [14] using sets A and C.

sum, defined as Y_L by Satchler [13]

$$Y_L = \sum_\alpha \frac{2(\beta_\alpha^L)^2}{(2L+1)E_\alpha}. \tag{12}$$

This quantity is important in the static polarization of nuclei. There is no collective theory for Y_L, but it can be guessed at using empirical data for low energy properties combined with eq. (9) to deduce high energy behavior. This piecemeal model was used in a theory of the ^{208}Pb optical potential [14], and the values of Y_L are plotted in fig. 6. The Green's function theory gives Y_L simply as the real part of the response at $E = 0$.

$$Y_L = \frac{\mathrm{Re}\langle(\mathrm{d}\rho_0/\mathrm{d}r)G(\mathrm{d}\rho_0/\mathrm{d}r)\rangle}{[R\int(\mathrm{d}\rho_0/\mathrm{d}r)^2 r^2 \mathrm{d}r]^2}. \tag{13}$$

The prediction of eq. (13) is also plotted in fig. 7, and we see that agreement is rather good. This is perhaps no more than a reflection that the RPA does not do badly on isoscalar properties for both low and high energies.

References

[1] G.F. Bertsch, Phys. Rev. Letters 31 (1973) 121.
[2] G.F. Bertsch and S.F. Tsai, to be published.
[3] D. Vautherin and D.M. Brink, Phys. Rev. C5 (1972) 626.
[4] A. Bohr, Mat. Fys. Medd. Dan. Vid. Selsk. 26 (1952) no. 14.
[5] L.J. Tassie, Aust. J. Phys. 9 (1956) 407.
[6] K. Itoh, M. Oyamada and Y. Torizuka, Phys. Rev. C2 (1970) 2181.
[7] T.J. Deal and S. Fallieros, Phys. Rev. C7 (1973) 1709.
[8] J.V. Noble, Annals of Physics 67 (1971) 98.
[9] G. Bertsch, to be published in Annals of Physics.
[10] M. Goldhaber and E. Teller, Phys. Rev. 74 (1948) 1046.
[11] H. Steinwedel, J.H.D. Jensen and P. Jensen, Phys. Rev. 79 (1950) 1019.
[12] W. Weng, T. Kuo and G. Brown, Phys. Letters 46B (1973) 329.
[13] G.R. Satchler, Nucl. Phys. A195 (1972) 1.
[14] C. Rao, M. Reeves and G. Satchler, Nucl. Phys. A207 (1973) 182.